Reversibly locking a protein fold in an active conformation with a disulfide bond: Integrin αL I domains with high affinity and antagonist activity *in vivo*

Motomu Shimaoka*†, Chafen Lu*‡, Roger T. Palframan*, Ulrich H. von Andrian*, Alison McCormack*, Junichi Takagi*, and Timothy A. Springer*§

The Center for Blood Research and Departments of *Pathology and †Anesthesia, Harvard Medical School, 200 Longwood Avenue, Boston, MA 02115

Contributed by Timothy A. Springer, March 15, 2001

The integrin αLβ2 has three different domains in its headpiece that have been suggested to either bind ligand or to regulate ligand binding. One of these, the inserted or I domain, has a fold similar to that of small G proteins. The I domain of the αM and α2 subunits has been crystallized in both open and closed conformations; however, the αL I domain has been crystallized in only the closed conformation. We hypothesized that the αL domain also would have an open conformation, and that this would be the ligand binding conformation. Therefore, we introduced pairs of cysteine residues to form disulfides that would lock the αL I domain in either the open or closed conformation. Locking the I domain open resulted in a 9,000-fold increase in affinity to intercellular adhesion molecule-1 (ICAM-1), which was reversed by disulfide reduction. By contrast, the affinity of the locked closed conformer was similar to wild type. Binding completely depended on Mg^{2+}. Orders of affinity were ICAM-1 > ICAM-2 > ICAM-3. The k_{on}, k_{off}, and K_D values for the locked open I domain were within 1.5-fold of values previously determined for the αLβ2 complex, showing that the I domain is sufficient for full affinity binding to ICAM-1. The locked open I domain antagonized αLβ2-dependent adhesion *in vitro*, lymphocyte homing *in vivo*, and firm adhesion but not rolling on high endothelial venules. The ability to reversibly lock a protein fold in an active conformation with dramatically increased affinity opens vistas in therapeutics and proteomics.

The integrin αLβ2 on leukocytes mediates adhesion and migration in immune responses within lymphoid organs and trafficking of leukocytes in inflammation and homing of lymphocytes within the body. αLβ2 binds multiple, related cell surface glycoprotein ligands that are members of the IgSF, including intercellular adhesion molecule-1 (ICAM-1), ICAM-2, and ICAM-3 (1). Adhesiveness of the extracellular domains of αLβ2 is rapidly and dynamically regulated by signals within the cell in a process termed inside-out signaling. Thus, αLβ2 can act as an adhesion servomotor controlled by antigen receptors and G protein-coupled chemoattractant receptors during immune responses and cell migration. Both clustering in the membrane (avidity regulation) and receptor conformational change (affinity regulation) have been proposed to regulate adhesiveness of αLβ2 (2–8).

Integrin αβ heterodimers have a complex domain organization (9). A ligand binding headpiece that contains domains from both subunits is connected by long C-terminal α and β subunit stalk regions to the membrane. An inserted domain (I domain) that is located in the headpiece of the αL subunit is implicated as a critical ligand binding site. However, a β-propeller domain in the αL subunit and an I-like domain in the β2 subunit also have been suggested to contribute to ligand binding (9). I domains from several different integrin α subunits have been crystallized. The I domain has a dinucleotide binding fold with a central hydrophobic β-sheet surrounded by amphipathic α-helices, and a metal ion-dependent adhesion site (MIDAS) on the ligand-binding face. Crystal structures for two different I domain conformations, termed open and closed, have been obtained for αM and α2 I domains, and it has been hypothesized that these represent the "high affinity" and "low affinity" conformations, respectively (10–12). The two conformers differ in the side chains that coordinate the Mg^{2+} ion in the MIDAS, which is hypothesized to make the Mg^{2+} ion in the open conformer more electrophilic for an acidic residue from the ligand. Also, in the open conformation, there is a 10-Å movement of the C-terminal α-helix down the body of the I domain and a large rearrangement and downward movement of the loop connecting this helix to the preceding β-strand. Small G proteins such as Ras are structurally related to I domains and exhibit similar alterations in Mg^{2+} ion coordination that are coupled to peptide backbone rearrangements (11).

Disulfides have previously been successfully used to restrict intramolecular mobility and probe conformational change in bacterial chemoreceptors (13, 14) and rhodopsin (15), as well as to increase the stability of proteins (16). However, efforts to lock in active conformations with disulfides have been challenging. Rhodopsin has thus far been locked only in the inactive form (15); the bacterial aspartate receptor has been locked in forms with up to 4-fold higher enzymatic activity and 8-fold higher affinity for aspartate (17).

The structure of the αL I domain has been determined only in the closed conformation (18); however, there is direct evidence for conformational change (19), and we hypothesized that the αL I domain might exist in an open conformation similar to that seen in crystal structures for αM (10) and α2 (12) I domains. We have introduced disulfide bonds into the αL I domain to lock it in the open or closed conformation and examined the consequences for cell adhesion (20, 21). Here we describe our methodology, directly demonstrate disulfide bond formation, measure the kinetics and affinity of soluble recombinant I domains locked in specific conformations for ICAM-1, ICAM-2, and ICAM-3, and investigate adhesion antagonism *in vitro* and *in vivo*. We demonstrate that the conformation of the αL I domain dramatically regulates affinity for ligand and that disulfide bond engineering has the potential to increase protein affinity many orders of magnitude more than previously achieved.

BIOCHEMISTRY

Abbreviations: I domain, inserted domain; ICAM, intercellular adhesion molecule; MIDAS, metal ion-dependent adhesion site; LFA-1, lymphocyte function-associated antigen-1; GFP, green fluorescent protein; PLN, peripheral lymph node.

‡Present address: Millennium Pharmaceuticals, 75 Sidney Street, Cambridge, MA 02139.

§To whom reprint requests should be addressed.

The publication costs of this article were defrayed in part by page charge payment. This article must therefore be hereby marked "*advertisement*" in accordance with 18 U.S.C. §1734 solely to indicate this fact.

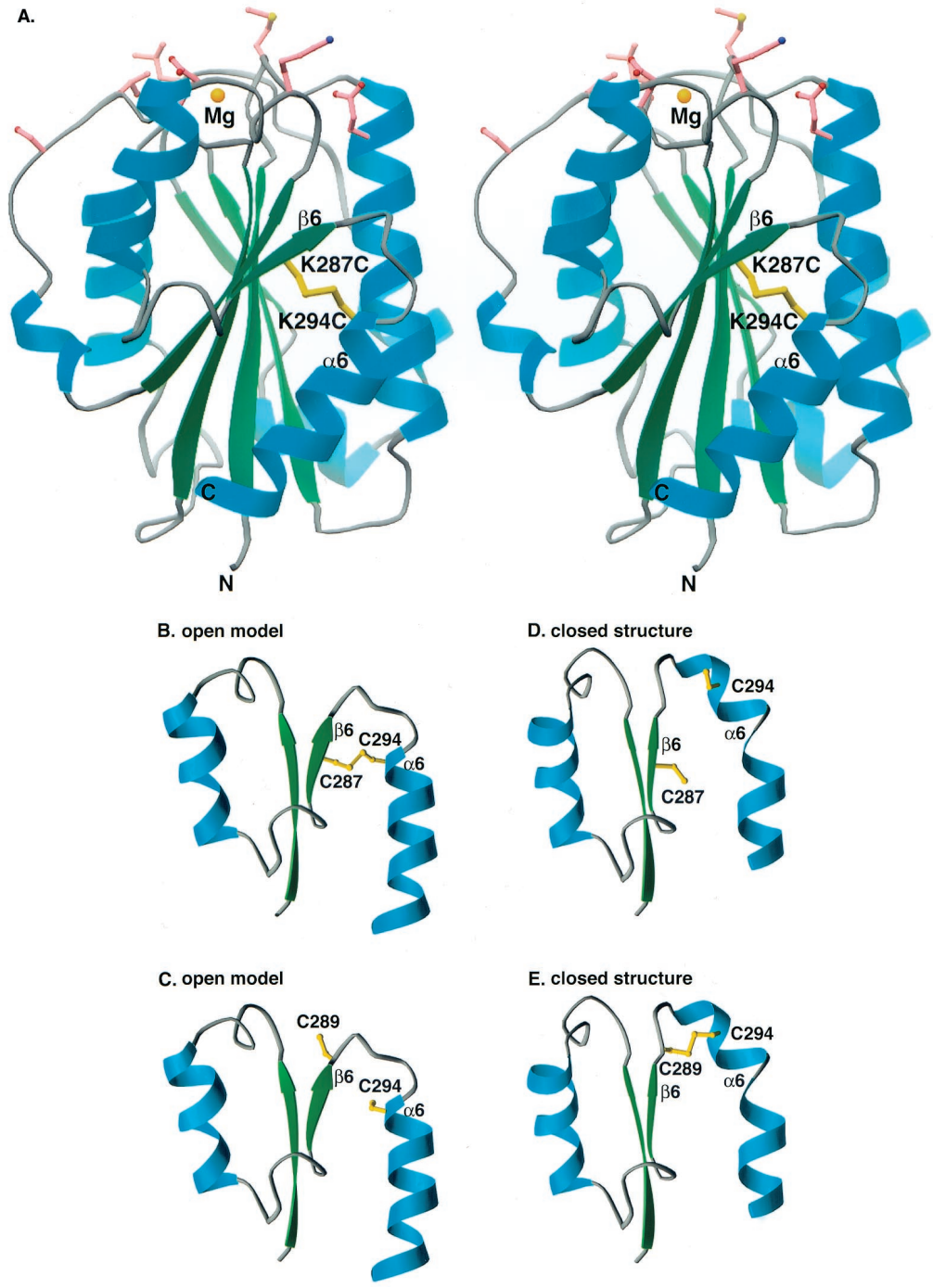

Fig. 1. Mutant αL I domains. (*A*) Stereodiagram of the high affinity model of the αL I domain, with mutations to introduce a disulfide bond. The side chains and disulfide bond of C287 and C294 are shown in yellow. The Mg^{2+} ion of the MIDAS is shown as a gold sphere. Side chains of residues important in binding to ICAM-1 and ICAM-2 are shown with rose-pink side chains and yellow sulfur, red oxygen, and blue nitrogen atoms. These residues, defined as important in species-specific binding to ICAM-1 (43) or by at least a 2-fold effect on binding to ICAM-1 or ICAM-2 upon mutation to alanine (44), are M140, E146, T175, L205, E241, T243, S245, and K263. Note that these residues surround the Mg^{2+} ion and are distant from the disulfide. (*B–E*) Predicted disulfide bonds that are selective for open or closed conformers of the αL I domain. The K287C/K294C mutation (*B* and *D*) and L289C/K294C mutation (*C* and *E*) were modeled in both open (*B* and *C*) and closed (*D* and *E*) I domain conformers. For clarity, only residues 254–305 of the models are shown. The four models were superimposed by using residues not involved in conformational shifts and are shown in exactly the same orientation. The downward movement of the α6 helix in *B* and *C* compared with *D* and *E* is readily apparent. Figure was prepared with RIBBONS (45).

Methods

A Model for the Open αL I Domain. I domains with the following Protein Data Bank identifiers were structurally superimposed by using Cα carbons, the three-dimensional MALIGN algorithm of MODELLER 4 (22) and a gap extension penalty of 1 Å: Mac-1, 1ido (10) and 1jlm (11); lymphocyte function-associated antigen-1 (LFA-1), 1lfa molecules A and B (18), 1zon and 1zop (23); and VLA-2, 1aox (24). The algorithm found 121 framework residues that were used for superposition. A second sequence and structure-based alignment also was made. The 1ido and 1jlm

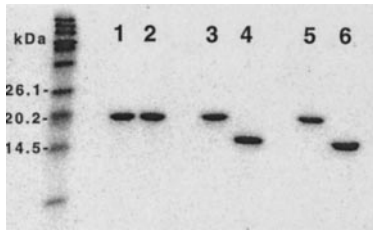

Fig. 2. SDS/PAGE of refolded I domains. Purified wild-type (lanes 1 and 2), open (lanes 3 and 4), and closed (lane 5 and 6) I domains (2.5 μg) treated in sample buffer containing 10 mM DTT (lanes 1, 3, and 5) or 10 mM iodoacetamide (lanes 2, 4, and 6) were subjected to SDS/18% PAGE and Coomassie blue staining.

structures were aligned by sequence, and the sequences of 1lfa molecule A and 1zon were aligned by structural similarity to 1jlm. Using the second alignment, the distances between all Cα carbons at equivalent sequence positions were calculated by using a Microsoft EXCEL spreadsheet (11). For use as templates for the high affinity αL I domain model, segments from 1lfa molecule A were chosen where differences between all four I domains were small or differences between 1lfa and 1jlm (closed αL and αM I domains) were greater than between 1ido and 1jlm (open and closed αM I domains). Segments from 1ido were chosen when differences between 1ido and 1jlm were greater than between 1lfa and 1jlm. Thus, the template used segments G128 to F136, M154 to L203, F209 to L234, T243 to I255, and E272 to A282 of 1lfa, and segments D140 to F156, G207 to T211, V238 to K245, R266 to R281, and R293 to K315 of 1ido. Models of a putative open form of αL were made with MODELLER 4 by using this template, the Mg^{2+} and water molecules 403 and 404 of 1ido, with heteroatom, water, and hydrogen input turned on, and dynamic Coloumb turned on. The resulting model (lfa_hi.063) followed the template Cα coordinates closely (rms = 0.12 Å). The QUACHK score (25) is excellent (−0.135 compared with −0.215 for the lfa-mac template, −0.08 for 1ido, and 0.0 for 1lfa). Models also were built in which cysteines were introduced (Fig. 1 *B–E*); however, it should be noted that all Cβ atom distances reported here are based on models or structures without introduced disulfides.

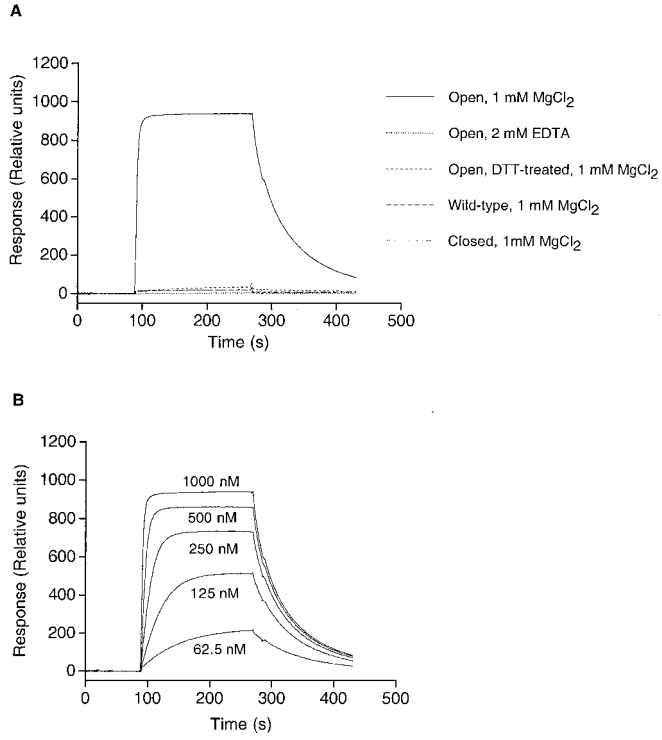

Fig. 3. I domain binding to ICAM-1 in BIAcore. (*A*) Overlay of representative sensorgrams recording interaction of I domains with ICAM-1. Soluble I domains (1 μM) were interacted with the extracellular fragment of ICAM-1 (46) immobilized on the sensorchip. (*B*) Overlay of sensorgrams of different concentrations of the open I domain in the presence of 1 mM $MgCl_2$.

Table 1. Kinetics of interaction of I domains with ICAM-1 in the presence of Mg^{2+}

I domain	k_{on}, $M^{-1}\cdot s^{-1}$	k_{off}, s^{-1}	K_D*, μM
Open	139,000 ± 8,000	0.0249 ± 0.0026	0.185 ± 0.012
Open + DTT	2,980 ± 440	3.86 ± 0.47	1,230 ± 90
Closed	2,110 ± 400	2.84 ± 0.27	1,760 ± 70
Closed + DTT	3,730 ± 370	3.25 ± 0.27	1,340 ± 100
Wild type	2,950 ± 440	5.55 ± 0.65	1,670 ± 100
Wild type + DTT	3,260 ± 290	4.72 ± 0.39	1,630 ± 190

*K_D was measured by Scatchard analysis of the amount of binding reached before the dissociation phase. These values are very close to those calculated from the k_{on} and k_{off} values shown above.

Prediction of Novel Disulfide Bonds. The 1lfa and 1zon structures and the lfa_hi.063 model were examined with SSBOND (26). Residues K287 and K294 in lfa_hi.063 and residues L289 and K294 in 1lfa and 1zon were found to have Cβ atom distances in the range between 3.41 and 4.25 Å that is favorable for disulfide bond formation.

Construction and Expression of the αL I Domains. Wild-type and mutant αL I-domains (G128-Y307) in expression vector pET11a (Novagen) were constructed by standard molecular biology techniques. Mutant and wild-type I domains were expressed in *Escherichia coli*, refolded, and purified as described (27) except 0.1 mM $CuSO_4$ and 0.1 mM *o*-phenanthroline were added during refolding to catalyze disulfide bond oxidation.

BIAcore. I domains, ICAMs, or BSA as control were covalently immobilized to the dextran surface of CM5 sensor chips via primary amino groups, using the amine coupling kit (BIAcore, Piscataway, NJ). Analytes were flowed over the sensor chip at 10 μl/min, 25°C. Tris-buffered saline containing either 1 mM $MgCl_2$, 1 mM $MnCl_2$ or 2 mM EDTA was used as running buffer, and 20 mM Tris (pH 8), 0.3 M NaCl, 20 mM EDTA was used to remove bound protein and regenerate the surface. Kinetics were analyzed by BIAEVALUATION 3.0 software. Analysis was done after subtracting bulk change and nonspecific binding. Unless otherwise stated, K_D was calculated by Scatchard plots using data at steady state. k_{off} was obtained by curve fitting of the dissociation phase using a 1:1 binding model. k_{obs} was obtained by curve

Table 2. Kinetics of interaction of designed open I domain with ligands

Immobilized ligand	Analyte	k_{on}, $M^{-1}\cdot s^{-1}$ $\times 10^{-5}$	k_{off}, s^{-1} $\times 10^{2}$	K_D*, nM
Open I domain	sICAM-1	1.07 ± 0.03	3.16 ± 0.26	258 ± 24
sICAM-1	Open I domain	1.39 ± 0.08	2.49 ± 0.26	185 ± 12
ICAM-1-Fc	Open I domain	1.18 ± 0.14	2.14 ± 0.17	173 ± 26
ICAM-2-Fc	Open I domain	0.26 ± 0.02	1.97 ± 0.31	605 ± 55
ICAM-3-Fc	Open I domain	0.18 ± 0.02	6.44 ± 0.97	4,320 ± 202

*K_D was measured as described in Table 1.

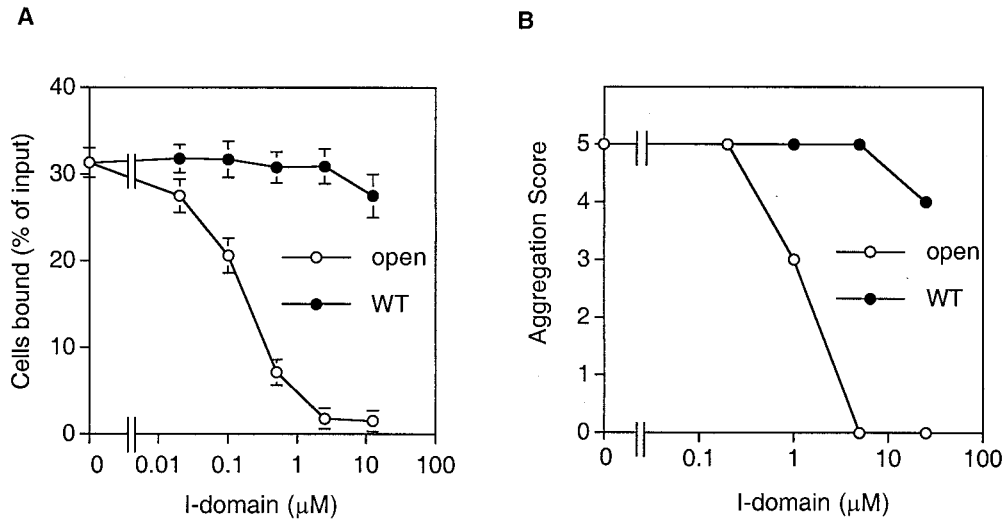

Fig. 4. Inhibition of adhesion *in vitro*. (*A*) Adhesion of K562 cells expressing wild-type (WT) LFA-1 to ICAM-1. Data are mean ± SEM of three independent experiments in duplicate. (*B*) Homotypic aggregation of murine EL-4 cells. Three independent experiments showed identical results.

fitting of the association phase and then k_{on} was calculated by using plots of k_{obs} vs. concentration.

Cell Adhesion to Immobilized ICAM-1. Adhesion of K562 cells expressing wild-type LFA-1 in 1 mM Mn^{2+} to ICAM-1 immobilized on 96-well plates (28) was carried out in the presence of the indicated concentration of I domains.

Homotypic Aggregation Assay. Phorbol 12-myristate 13-acetate-induced homotypic aggregation of murine EL-4 cells was carried out and scored as described (29).

Homing Assay. Homing assay was as described (30). Mice were injected with a bolus of either saline vehicle, designed open I domain or wild-type I domain (50 μg/g body weight). Mice were injected 3 min later with a bolus of 20×10^6 donor green fluorescent protein-positive (GFP^+) T lymphocytes (31), followed by constant infusion for 20 min with saline vehicle, or locked open or wild-type I domain (3.7 μg/g body weight/min). Peripheral lymph nodes (PLNs) were removed and GFP^+ T lymphocytes in cell suspensions were identified by flow cytometry.

Intravital Microscopy. Lymphocyte traffic on high endothelial venules of subiliac PLN was directly observed by intravital microscopy as described (30). After recording the behavior of a control injection of GFP^+ T lymphocytes under baseline conditions, wild-type or locked open I domain (10 μg/g body weight) was infused, and behavior of a second bolus of GFP^+ T lymphocytes was recorded. Data were analyzed off-line as described (30).

Results

Design of I Domains Locked in Open and Closed Conformations. We designed disulfide bonds to lock the αL I domain either in the closed conformation or in the hypothetical open conformation. The open conformation of the αM I domain (1ido) seen in a crystal structure with a ligand-mimetic lattice contact (10) was used to model the open conformation of the αL I domain (Fig. 1*A*). The template for this model consisted of segments of the open αM I domain structure in regions where the Cα backbone differed significantly from the closed αM I domain structure and segments of the closed αL I domain structure (18) elsewhere. The open αL I domain model and two closed αL I domain structures were examined with the program SSBOND (26) to find positions where cysteine pairs could be introduced to form conformation-specific disulfides. One pair of residues (K287 and K294) in the open model, and one pair of residues (L289 and K294) in the closed structures, underwent large movements between the two conformers, such that after substitution with cysteine, disulfide bond formation could occur only in one conformer (Fig. 1 *B–E*). These disulfides bridge the C-terminal α-helix to the preceding β-strand and lock the connecting loop in the two alternative conformations seen in the open and closed structures.

Expression of I Domains and Formation of Disulfide Bonds. Expression in *E. coli*, refolding, and formation of disulfide bonds in soluble I domains are described in *Methods*. Purified I domains were monomeric as shown by gel filtration. Intramolecular disulfide bond formation was confirmed by the decrease in mobility in SDS/PAGE seen after reduction for the open and closed I domains (Fig. 2, lanes 3–6) but not for the wild-type I domain (Fig. 2, lanes 1 and 2).

Kinetics and Equilibria of αL I Domain Binding to ICAMs. Binding of the αL I domains to the IgSF ligand ICAM-1 was measured with BIAcore. The designed open I domain showed strong binding to immobilized ICAM-1 in the presence of Mg^{2+}, whereas the designed closed and wild-type I domains showed very weak interaction with ICAM-1 (Fig. 3*A*). Wild-type and designer I domains at the same protein concentration bound identically to mAb TS1/22 to the αL I domain (not shown). Ligand binding by the designed open I domain was abolished by reduction of the disulfide bond with DTT (Fig. 3*A*). Binding also was abolished by EDTA (Fig. 3*A*) and thus depended on Mg^{2+}, suggesting that binding of the open I domain is mediated by the MIDAS.

Kinetic constants were measured from the association and dissociation phase in BIAcore; K_D was measured by Scatchard plots of binding at plateau (Fig. 3*B*) and was in good agreement with calculation of K_D from k_{off}/k_{on}. The affinity of the open I domain for ICAM-1 is 9,000-fold higher than that of the wild-type I domain (Table 1). Both an increase in k_{on} and a decrease in k_{off} contributed to this dramatic increase in affinity (Table 1). These results were confirmed by using the reverse orientation with the I domain immobilized on the sensor chip (Table 2). Increased affinity of the open I domain was completely reversed by reduction of the disulfide bond (Table 1). By contrast, the K_D of the closed I domain was similar to that of wild type and was not changed by reduction with DTT (Table 1).

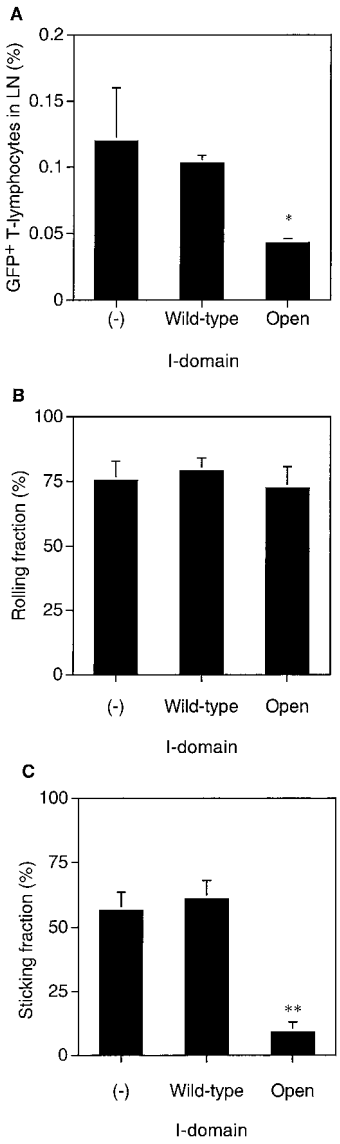

Fig. 5. Antagonism of LFA-1-dependent T lymphocyte adhesion *in vivo*. (*A*) Homing to PLNs. Data are expressed as mean ± SEM ($n = 3$). *, $P < 0.05$ vs. wild type. (*B* and *C*) Effect of I domains on T lymphocyte rolling and sticking in high endothelial venules of subiliac PLN. Data are mean ± SEM (a total of 15 vessels in four mice were analyzed). **, $P < 0.01$ vs. control or wild type.

Thus, conformational change dramatically regulates the affinity of the αL I domain for ligand.

We compared binding to three distinct LFA-1 ligands, ICAM-1, ICAM-2, and ICAM-3. The open I domain bound well not only to ICAM-1 but also to ICAM-2 and ICAM-3 (Table 2), whereas the wild-type I domain bound poorly to all three ligands (data not shown). The affinity is highest for ICAM-1 and lowest for ICAM-3. These results are consistent with the previous conclusion from cell adhesion assays that LFA-1 binds to ICAM-1 stronger than ICAM-2 or ICAM-3 (32).

Antagonist Activity of Locked Open I Domain. The potential to antagonize adhesion with locked open I domains was examined *in vitro* and *in vivo*. Open I domains potently antagonized cell adhesion through LFA-1 to ICAM-1 (Fig. 4*A*). Although the wild-type I domain can inhibit adhesion (33), it was much weaker than the open I domain (Fig. 4*A*). Furthermore, the open, but not wild-type, I domain potently blocked LFA-1- and ICAM-1-dependent homotypic aggregation of mouse EL-4 T-lymphoma cells (29) (Fig. 4*B*). BIAcore experiments confirmed that the affinity of the locked open human αL I domain for murine ICAM-1 was comparable to that for human ICAM-1, with K_D of 191 nM.

Lymphocyte homing to PLNs depends on an initial step of rolling through L-selectin and a subsequent step of chemokine-triggered firm adhesion through LFA-1 (1). I domains were infused intraarterially, and homing of GFP transgene-expressing, naïve T lymphocytes was examined (30). Homing of lymphocytes to PLNs was significantly reduced ($P < 0.05$) after treatment with the locked open I domain compared with the wild-type I domain (Fig. 5*A*). Consistent with these results, more lymphocytes remained in the circulation in locked open I domain-treated mice than in wild-type I domain-treated mice (10.0×10^5/ml and 5.7×10^5/ml, respectively, $P < 0.05$). The behavior of lymphocytes in high endothelial venules in PLNs was directly observed by using intravital microscopy (34). Rolling was unaffected by either type of I domain (Fig. 5*B*). By contrast, the locked open, but not wild-type, I domain significantly inhibited the conversion of rolling cells to firmly adherent cells (Fig. 5*C*). Thus, the locked open I domain specifically blocked LFA-1-dependent T lymphocyte sticking and did not interfere with selectin-dependent T lymphocyte rolling.

Discussion

Our work with designed I domains locked in different conformational states directly demonstrates the importance of conformation for regulating ligand binding by integrins. Locking the I domain open with a disulfide bond bracketing the β6-α6 loop increased affinity for ICAM-1 by 9,000-fold and also greatly increased binding to ICAM-2 and ICAM-3. After reduction of this disulfide, the affinity was reduced to a level comparable to wild type. Furthermore, the affinities of the wild-type, locked closed, and reduced locked open mutants were comparable. These findings strongly suggest that the isolated wild-type I domain exists predominantly in the closed conformation, and that this is the low energy conformation. Furthermore, because only the conformation of the β6-α6 loop is directly restrained by the disulfide, our results show that reshaping of this loop and the concomitant downward movement of the C-terminal α-helix are fully sufficient for rearrangement of the MIDAS into a ligand binding configuration. Thus, in intact integrins, a downward pull on the C-terminal α-helix of the I domain exerted by neighboring domains would be sufficient to open the ligand binding site. In intact integrins, the C terminus of the I domain connects to the predicted β-propeller domain, and this connection is near the β-subunit I-like domain (35). Interactions with these neighboring domains may stabilize the open conformation of the I domain in intact αLβ2. Measurements on active αLβ2 in solution or on the surface of cells show K_D values of 60 nM to 500 nM (2, 36, 37). Remarkably, the published parameters for αLβ2 binding to ICAM-1 determined by BIAcore, $k_{on} = 2.24 \times 10^5$ $M^{-1}s^{-1}$, $k_{off} = 0.0298\ s^{-1}$, and $K_D = 133$ nM (37) are within 1.2- to 1.6-fold of the values here for open I domain binding to ICAM-1, but differ greatly from the values for the wild-type and locked closed I domains. The similarity in these values strongly suggest that a single integrin domain, when in an appropriate conformation, can be sufficient for full ligand binding activity. The marked increase in k_{on} for the locked open I domain is compatible with the idea that for the native αL I domain, conformational opening usually would precede binding to ICAM-1. On the other hand, the ability to detect ligand binding by the locked closed I domain suggests that ICAM-1 binding could precede conformational opening, albeit with a markedly lower k_{on} than for a preopened I domain.

The locked open and closed αL I domains described here have previously been studied expressed on the cell surface, either as isolated I domains with artificial transmembranous and cytoplasmic domains or within αLβ2 heterodimers (20, 21). In both

contexts, the locked open I domains were as active in mediating cell adhesion as maximally activated wild-type $\alpha L\beta 2$. By contrast, the locked closed I domain constructs were inactive and completely resistant to activating stimuli. Taken together with the measurements on affinity reported here, these studies suggest that conformational change and affinity regulation are required for activation of adhesiveness through $\alpha L\beta 2$.

Cellular treatments that increase the rate of diffusion of $\alpha L\beta 2$ augment adhesion through $\alpha L\beta 2$ and both increase in the rate of diffusion and adhesiveness are associated with clustering of $\alpha L\beta 2$ in the membrane; therefore, it has been suggested that clustering can augment adhesiveness through avidity modulation in the absence of affinity modulation (4–6, 8, 38). Furthermore, binding of dimeric or multimeric ICAM-1 and binding of activation-dependent mAB to cell surface $\alpha L\beta 2$ have been reported after some but not other types of stimulation that augment adhesiveness through $\alpha L\beta 2$ (3, 4, 38). However, the failure to detect binding of ICAM-1 to cells under certain types of conditions that activate adhesiveness could reflect a lack of sensitivity to intermediate levels of $\alpha L\beta 2$ affinity, rather than a lack of affinity regulation. We have shown here that the difference in affinity between the open and closed conformations is quite large, 10^4. This finding corresponds to a requirement of 5.4 kcal to stabilize the open conformation of the I domain. In native $\alpha L\beta 2$, this stabilization would be contributed by interaction with neighboring domains, such as the I-like and β-propeller domains. Multiple conformational states of $\alpha L\beta 2$ may exist, with different amounts of stabilization of the open I domain conformation, and hence different affinities for ICAM-1. The K_D of 200 nM of the locked open I domain is just barely within the range that is detectable by conventional assays for ligand binding to cells. The K_D of 2 mM of the closed conformation is quite low and is barely detectable even with BIAcore assays. A hypothetical intermediate affinity state of 20 μM would not be detectable by ligand binding to cells, but might be sufficient to activate cell adhesion. Therefore, a definitive resolution of the contributions of avidity and affinity regulation to the adhesiveness of $\alpha L\beta 2$ cannot occur until much more sensitive assays are developed for binding of monomeric ICAM-1 to cell surface $\alpha L\beta 2$.

We have extended the approach described here to another I domain, that of the αM integrin subunit, and have found multiple positions in both the αL and αM domains where disulfide bonds can be introduced that stabilize the open conformation and increase affinity for ligand (M.S. and T.A.S., unpublished work). Using a different approach, we previously have used computational design to find mutations in the hydrophobic core of the αM I domain that stabilize the open and closed conformations (39). From eight to 13 substitutions in the hydrophobic core were used to stabilize the open conformation (39). The introduction of a disulfide bond into the αM I domain appears to be similarly effective in increasing ligand binding activity as measured both in adhesion assays and in BIAcore (M.S. and T.A.S., unpublished work).

Many biologically and pharmaceutically important proteins exist in two different three-dimensional conformations, and like integrins, have functions that are regulated by conformational change, e.g., G proteins, kinases, and G protein-coupled receptors (40). Therefore, the ability to reversibly lock a protein fold in an active conformation opens vistas in therapeutics and proteomics. As one example of this, integrins that contain I domains are very important therapeutic targets in inflammation, autoimmunity, and transplantation (41). We have demonstrated here that locked open I domains are potent adhesion antagonists, both *in vitro* and *in vivo*. The locked open αL I domain inhibited lymphocyte homing. Furthermore, it inhibited the transition of lymphocytes in lymphoid high endothelial venules from rolling adhesion to firm adhesion, but did not inhibit rolling adhesion. These steps are known to depend on $\alpha L\beta 2$ and L-selectin, respectively (1, 42), demonstrating the high specificity of the locked open I domain *in vivo*. Our results suggest that locked open I domains can be used to demonstrate the importance of specific molecular targets in disease processes and are therapeutic candidates. Receptors locked in high affinity conformations offer many advantages, including discrimination between drugs that bind to ligand binding and allosteric sites (20). Furthermore, antibodies can be rationally obtained that are specific for activated protein conformations for use in diagnosis and treatment of disease.

We thank Michael Dustin and Robert Liddington for reviewing the manuscript, Guiying Cheng and Annmarie Hayes for technical assistance, and Susanne Curry for secretarial assistance. This work was supported by National Institutes of Health Grants CA31798, HL54936, and HL62524 and by The Wellcome Trust.

1. Springer, T. A. (1994) *Cell* **76,** 301–314.
2. Lollo, B. A., Chan, K. W. H., Hanson, E. M., Moy, V. T. & Brian, A. A. (1993) *J. Biol. Chem.* **268,** 21693–21700.
3. Constantin, G., Majeed, M., Giagulli, C., Piccib, L., Kim, J. Y., Butcher, E. C. & Laudanna, C. (2000) *Immunity* **13,** 759–769.
4. Ganpule, G., Knorr, R., Miller, J. M., Carron, C. P. & Dustin, M. L. (1997) *J. Immunol.* **159,** 2685–2692.
5. McDowall, A., Leitinger, B., Stanley, P., Bates, P. A., Randi, A. M. & Hogg, N. (1998) *J. Biol. Chem.* **273,** 27396–27403.
6. Krauss, K. & Altevogt, P. (1999) *J. Biol. Chem.* **274,** 36921–36927.
7. Stewart, M. & Hogg, N. (1996) *J. Cell. Biochem.* **61,** 554–561.
8. van Kooyk, Y., van Vliet, S. J. & Figdor, C. G. (1999) *J. Biol. Chem.* **274,** 26869–26877.
9. Humphries, M. J. (2000) *Biochem. Soc. Trans.* **28,** 311–339.
10. Lee, J.-O., Rieu, P., Arnaout, M. A. & Liddington, R. (1995) *Cell* **80,** 631–638.
11. Lee, J.-O., Bankston, L. A., Arnaout, M. A. & Liddington, R. C. (1995) *Structure (London)* **3,** 1333–1340.
12. Emsley, J., Knight, C. G., Farndale, R. W., Barnes, M. J. & Liddington, R. C. (2000) *Cell* **101,** 47–56.
13. Falke, J. J. & Koshland, D. E., Jr. (1987) *Science* **237,** 1596–1600.
14. Falke, J. J. & Kim, S. H. (2000) *Curr. Opin. Struct. Biol.* **10,** 462–469.
15. Yu, H., Kono, M. & Oprian, D. D. (1999) *Biochemistry* **38,** 12028–12032.
16. Mansfeld, J., Vriend, G., Dijkstra, B. W., Veltman, O. R., Van den Burg, B., Venema, G., Ulbrich-Hofmann, R. & Eijsink, V. G. H. (1997) *J. Biol. Chem.* **272,** 11152–11156.
17. Chervitz, S. A. & Falke, J. J. (1995) *J. Biol. Chem.* **270,** 24043–24053.
18. Qu, A. & Leahy, D. J. (1995) *Proc. Natl. Acad. Sci. USA* **92,** 10277–10281.
19. Huth, J. R., Olejniczak, E. T., Mendoza, R., Liang, H., Harris, E. A., Lupher, M. L., Jr., Wilson, A. E., Fesik, S. W. & Staunton, D. E. (2000) *Proc. Natl. Acad. Sci. USA* **97,** 5231–5236.
20. Lu, C., Shimaoka, M., Ferzly, M., Oxvig, C., Takagi, J. & Springer, T. A. (2001) *Proc. Natl. Acad. Sci. USA* **98,** 2387–2392.
21. Lu, C., Shimaoka, M., Zang, Q., Takagi, J. & Springer, T. A. (2001) *Proc. Natl. Acad. Sci. USA* **98,** 2393–2398.
22. Sali, A. & Blundell, T. L. (1993) *J. Mol. Biol.* **234,** 779–815.
23. Qu, A. & Leahy, D. J. (1996) *Structure (London)* **4,** 931–942.
24. Emsley, J., King, S. L., Bergelson, J. M. & Liddington, R. C. (1997) *J. Biol. Chem.* **272,** 28512–28517.
25. Vriend, G. (1990) *J. Mol. Graph.* **8,** 52–56.
26. Hazes, B. & Dijkstra, B. W. (1988) *Protein Eng.* **2,** 119–125.
27. Legge, G. B., Kriwacki, R. W., Chung, J., Hommel, U., Ramage, P., Case, D. A., Dyson, H. J. & Wright, P. E. (2000) *J. Mol. Biol.* **295,** 1251–1264.
28. Lu, C. & Springer, T. A. (1997) *J. Immunol.* **159,** 268–278.
29. Johnston, S. C., Dustin, M. L., Hibbs, M. L. & Springer, T. A. (1990) *J. Immunol.* **145,** 1181–1187.
30. Stein, J. V., Rot, A., Luo, Y., Narasimhaswamy, M., Nakano, H., Gunn, M. D., Matsuzawa, A., Quackenbush, E. J., Dorf, M. E. & von Andrian, U. H. (2000) *J. Exp. Med.* **191,** 61–76.
31. Manjunath, N., Shankar, P., Stockton, B., Dubey, P. D., Lieberman, J. & von Andrian, U. H. (1999) *Proc. Natl. Acad. Sci. USA* **96,** 13932–13937.
32. de Fougerolles, A. R. & Springer, T. A. (1992) *J. Exp. Med.* **175,** 185–190.
33. Randi, A. M. & Hogg, N. (1994) *J. Biol. Chem.* **269,** 12395–12398.
34. von Andrian, U. H. (1996) *Microcirculation* **3,** 287–300.
35. Zang, Q., Lu, C., Huang, C., Takagi, J. & Springer, T. A. (2000) *J. Biol. Chem.* **275,** 22202–22212.
36. Woska, J. R., Jr., Morelock, M. M., Jeanfavre, D. D. & Bormann, B. J. (1996) *J. Immunol.* **156,** 4680–4685.
37. Labadia, M. E., Jeanfavre, D. D., Caviness, G. O. & Morelock, M. M. (1998) *J. Immunol.* **161,** 836–842.
38. Stewart, M. P., Cabanas, C. & Hogg, N. (1996) *J. Immunol.* **156,** 1810–1817.
39. Shimaoka, M., Shifman, J. M., Jing, H., Takagi, J., Mayo, S. L. & Springer, T. A. (2000) *Nat. Struct. Biol.* **7,** 674–678.
40. Bohm, A., Gaudet, R. & Sigler, P. B. (1997) *Curr. Opin. Struct. Biol.* **8,** 480–487.
41. Harlan, J. M., Winn, R. K., Vedder, N. B., Doerschuk, C. M. & Rice, C. L. (1992) in *Adhesion: Its Role in Inflammatory Disease*, eds. Harlan, J. R. & Liu, D. (Freeman, New York), pp. 117–150.
42. Warnock, R. A., Askari, S., Butcher, E. C. & von Andrian, U. H. (1998) *J. Exp. Med.* **187,** 205–216.
43. Huang, C. & Springer, T. A. (1995) *J. Biol. Chem.* **270,** 19008–19016.
44. Edwards, C. P., Fisher, K. L., Presta, L. G. & Bodary, S. C. (1998) *J. Biol. Chem.* **273,** 28937–28944.
45. Carson, M. (1997) *Methods Enzymol.* **277,** 493–505.
46. Marlin, S. D., Staunton, D. E., Springer, T. A., Stratowa, C., Sommergruber, W. & Merluzzi, V. (1990) *Nature (London)* **344,** 70–72.